Electronic Supplementary Material (ESI) for Physical Chemistry Chemical Physics

Supplementary Information

Heterogeneous nanotribological response of polymorphic self-assembled monolayers arising from domain and phase dependent friction

Markos Paradinas,[1*] *Carmen Munuera,*[1†] *Christophe Silien,*[2§] *Manfred Buck*[2] *and Carmen Ocal*[1*]

[1] Institut de Ciència de Materials de Barcelona (ICMAB-CSIC), 08193-Bellaterra, Spain

[2]EaStCHEM School of Chemistry, University of St. Andrews, North Haugh, St. Andrews KY169ST, UK

*mparadinas@icmab.es, *cocal@icmab.es

Present Addresses

[†]present address: Instituto de Ciencia de Materiales de Madrid (ICMM-CSIC), Cantoblanco 28049 Madrid, Spain

[§]present address: Department of Physics and Energy, and Materials and Surface Science, University of Limerick, Ireland.

1. Solitons and Vacancy Islands.

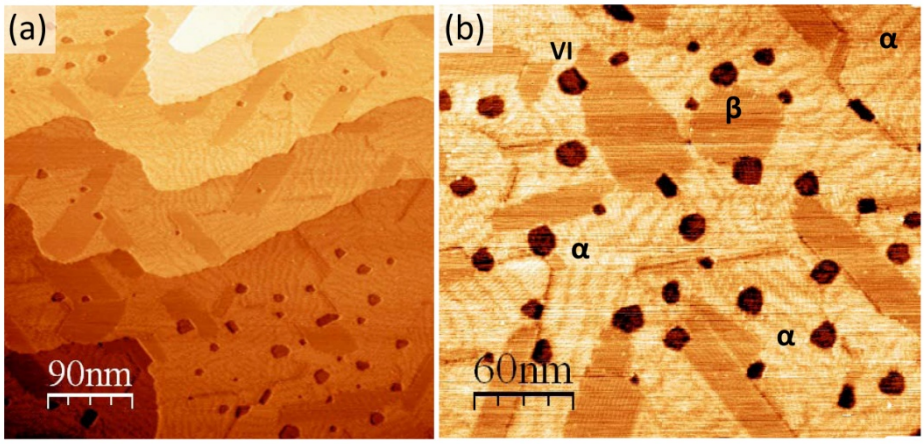

Figure S1. Scanning Tunneling Microscopy images of a BP4 SAM on Au(111). Images (a) and (b) at different magnifications show the two coexisting structures with the α-phase appearing brighter than the β-phase at each terrace. One β domain and three rotated domains of α have been labeled in (b). The rippled appearance of the α-phase is due to the reported solitons or domain walls, which appear to release stress and stabilize the adlayer. Different orientations of the domain walls in the α-phase are discernible. Running preferentially along the $< 11\bar{2} >$ directions they reflect the symmetry of the substrate and, thus, facilitate to identify the orientation of α-phase domains. Dark pits are the vacancy islands (VI) typical for SAMs on Au(111). U= 0.8 V, I=100 pA.

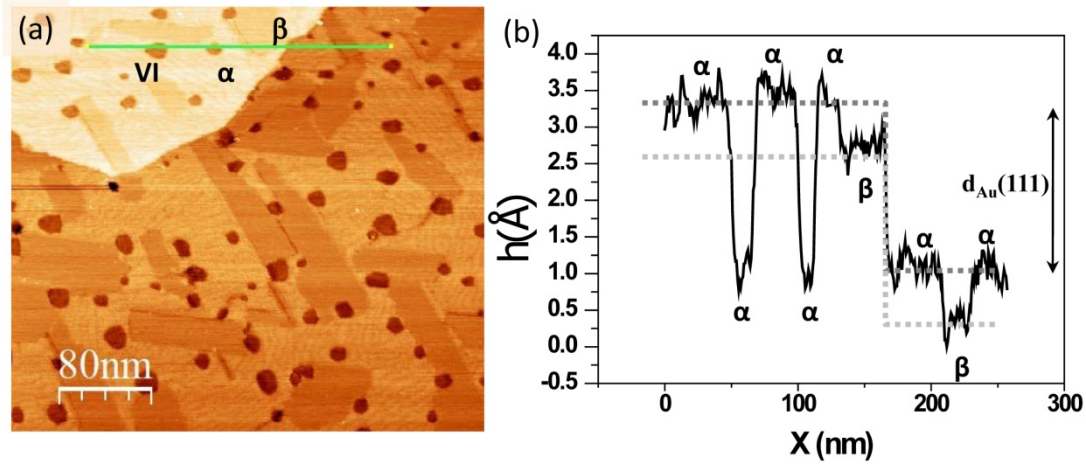

Figure S2. Vacancy islands analysis by Scanning Tunneling Microscopy. Analysis of heights in STM images of BP4 SAMs on Au(111). (a) Constant current STM images recorded at U= 0.8 V, I=100 pA. (b) height profile along the line indicated in the image. The black and grey dashed lines in (b) reproduce ideal Au(111) steps vertically shifted by the height difference between phases. The profile highlights that the depth of the vacancy island (VI) is identical to the step height $d_{Au}(111)$ of the Au substrate, i.e., both VIs and the surrounding area are covered by the α-phase. As evidenced, β regions lie lower than αregions on the same terrace. As a consequence when a β region is on the lower side of a step and an α region on the upper side, the step looks larger than $d_{Au}(111)$ whereas it looks lower in the opposite case, i.e., β on the upper terrace and α on the lower one.

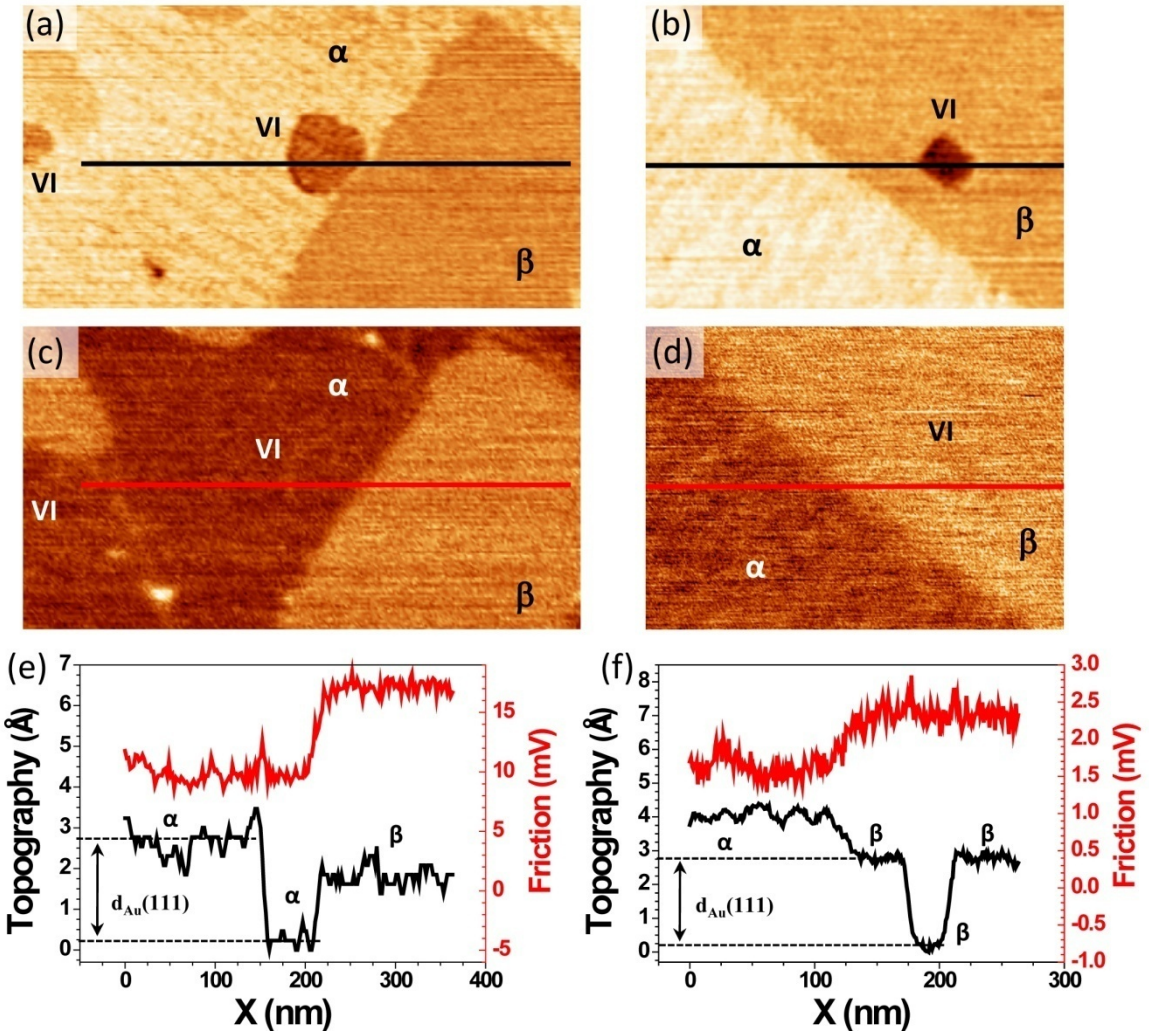

Figure S3. Vacancy islands analysis by Scanning Force Microscopy. Contact mode SFM data of BP4 SAM on Au(111). Topographic images in (a) and (b) have been chosen to show two surface regions in which α and β-phases coexist on the same atomically flat Au(111) terrace. These regions also include some vacancy islands (VI). The corresponding friction maps (c) and (d) are calculated as described in the text and show the contrast in friction expected between phases (1.6±0.2) with lower (darker) and higher (lighter) friction for α and β, respectively. Topographic and friction profiles in (e) and (f) correspond to the lines indicated in the respective images. The Au(111) step height $d_{Au}(111)$ is marked and serves as reference for phase dependent height differences. The VIs in (a) present the same friction contrast as the α-phase (c) and have a depth equal to $d_{Au}(111)$ relative to this phase, as seen in (e) for the VI at the image center. Conversely, as can be seen in (f) the VI observed in (b) presents the same friction contrast of the β-phase in which is embeded and, therefore, has also a depth equal to $d_{Au}(111)$.

Note: While regions as that in (a) with VI within α or at the boundary between α and β were commonly found, VI within β regions were rarely observed (<1% of the total VIs observed for three different BP4 SAMs and more than hundred different surface regions).

2. Adhesion force spectroscopy

Adhesion force (AF) maps in this work are based on the direct determination of the pull off force at each point of the scanned surface by withdrawing the SFM tip along the direction normal to the surface until the tip went out (snaps out) of contact. Therefore, AF in nN units was estimated as illustrated by the typical example shown in Fig. S4 and was recorded at each surface point in a second pass image to get AF maps on the very same surface locations as morphology and lateral force images (see Fig. 4 of the manuscript).

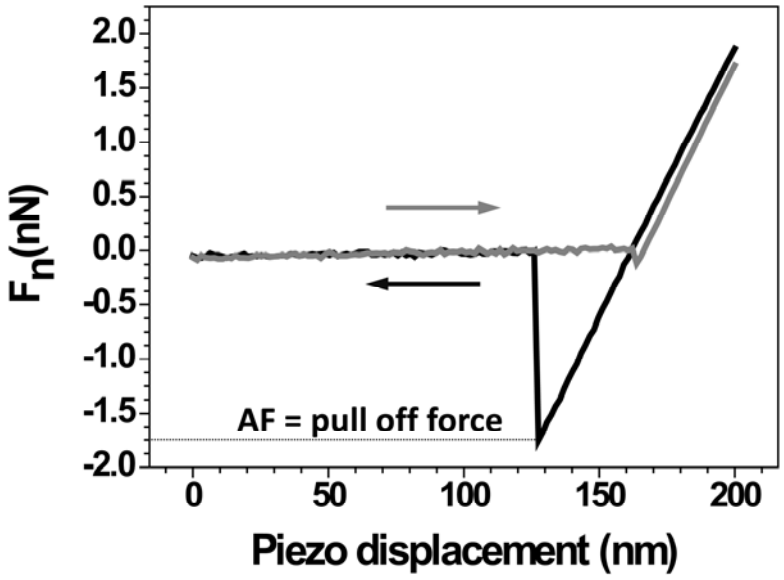

Figure S4. Adhesion force spectroscopy. Typical force versus distance performed on top of the BP4 SAM and used to determine adhesion force (AF) from the pull off force or snaps out of the tip in the retrace path. The procedure was performed at every point of the scanned surface area.

3. Friction anisotropy and friction asymmetry.

The reported friction anisotropy (AN) and friction asymmetry (AS) effects were verified in many different regions of three different samples of BP4 on Au(111). We present here a series of selected examples in which both AN and AS are seen by showing the lateral force images (forward and backward) and the corresponding friction image. The local friction signal is defined as half the amplitude of the so called friction loop, $F = ½(F_{lf} - F_{lb})$, where F_{li} is the lateral force signal of the forward (i=f) and the corresponding backward (i=b) scans. Applying this line by line procedure to the complete lateral force images leads to the friction maps shown in the figures. Friction anisotropy (AN) refers to the variation of the friction coefficient (μ) with the relative orientation of sliding surfaces and is commonly correlated with the azimuthal orientation of a crystalline surface. As a consequence AN

anisotropy is observed as a different contrast in a friction image, see for instance $F(\beta_1) \neq F(\beta_2)$ in Figure S5 or $F(\alpha_1) \neq F(\alpha_2)$ in Figure S6. On the other hand, AS, also called directional *dependence of friction,* arises from a direction dependent (asymmetric) surface potential, i.e. opposite for a change of 180º in direction. In such a case,$|F_{lf}(0^\circ)| = |F_{lb}(180^\circ)|$ and $|F_{lf}(180^\circ)| = |F_{lb}(0^\circ)|$, i.e., $F(\beta_1) = F(\beta'_1)$,and therefore AS is only observed in separate lateral force images (see for instance β_1 and β' in figures S6 and S7).

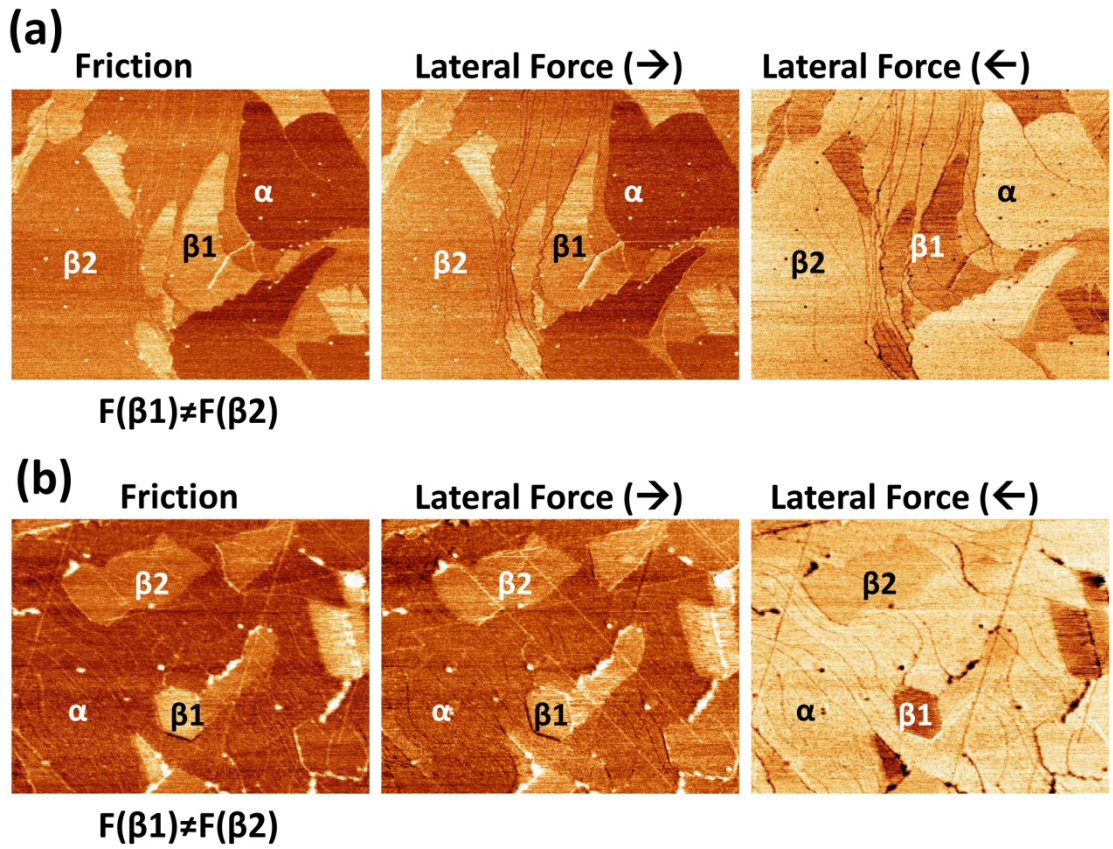

Figure S5. Friction Force Microscopy. Friction and lateral force images (forward and backward) of two different regions of the same BP4 SAM on Au(111). Lateral horizontal scales are 1950nm (a) and 1200nm (b). Cantilever stiffness k= 0.05 N/m. $F(\beta_1) \neq F(\beta_2)$ in the friction images (left panels) is a clear signature of friction anisotropy.

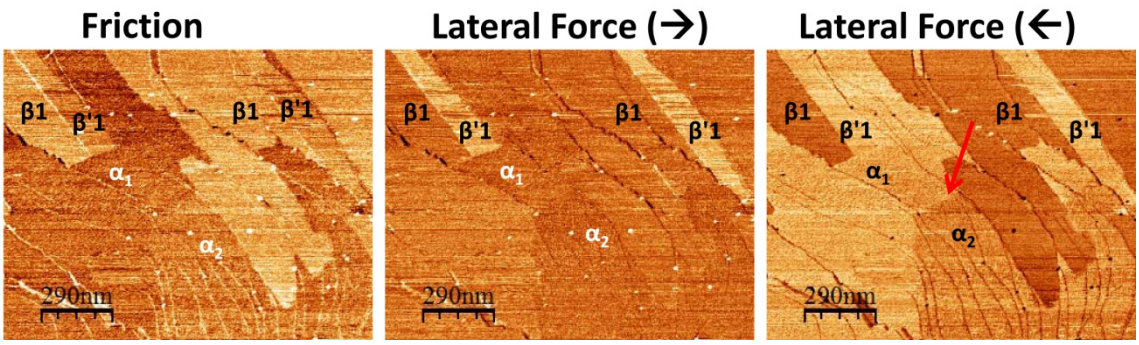

Figure S6. Scanning Force Microscopy. Friction and lateral force images (forward and backward) of a BP4 SAM on Au(111). Cantilever stiffness k= 0.05N/m. Observation of domains with equal or nearly equal friction values but clear contrast in both lateral force images (forward and backward) is indication of friction asymmetry. For soft cantilevers as the one employed in this particular case, contrast in the α-phase is also observed. This is particularly clear in the lateral force (←) image where the boundary between two α domains on the same surface terrace as indicated by the red arrow.

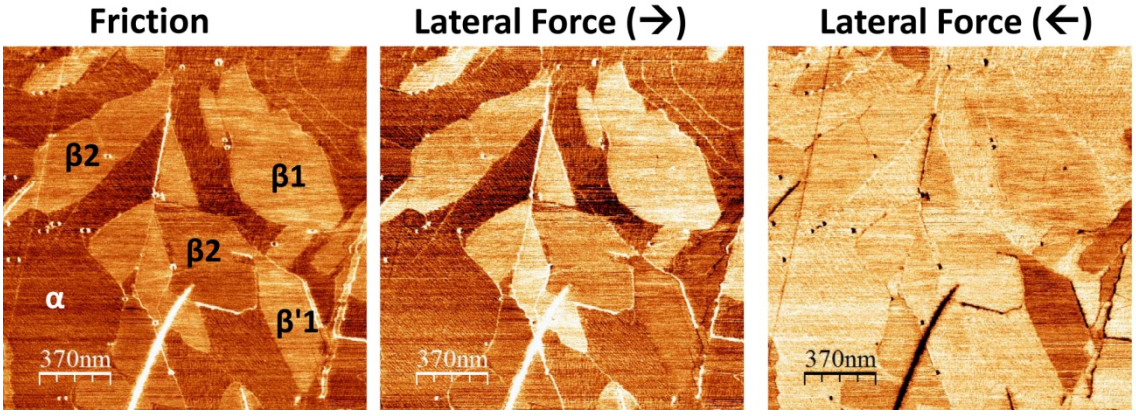

Figure S7. Friction Force Microscopy. Friction and lateral force images (forward and backward) of a different sample of BP4 SAM on Au(111). Cantilever stiffness k= 0.2 N/m. In this case we illustrate how the lateral heterogeneity in friction, at the scale of hundreds of nanometers, arises for differences in friction coming from the presence of different domains of the same structural phase. Note: the bright/dark line at the bottom of the images comes from a substrate scratch.